Impact of PEGMA on transport and co-transport of methanol and acetate in PEGDA-AMPS cation exchange membranes

Jung Min Kim[1], Antara Mazumder[1], Jing Li[1], Zhihua Jiang[1], Bryan S. Beckingham[1,*]

[1]Department of Chemical Engineering, Auburn University, Auburn, AL 36849, United States

*Corresponding Author: Tel: +1 (334) 844-2036

E-mail Address: bsb0025@auburn.edu (Bryan S. Beckingham)

Abstract.

Understanding multi-component transport behavior in membranes with varied internal structures and functionalities is critical for the rational design of membranes that will be challenged with the separation of, or come in contact with, multi-component solutions. One interesting application is ion exchange membranes for CO_2 reduction cells as these membranes interact with multiple CO_2 reduction products (e.g. methanol and acetate) whose permeation must be controlled, as they readily oxidize back to CO_2 and by-products in the anode chamber. Previously, the co-transport behavior of methanol and acetate in membranes with various pendant groups, such as sulfonate ($-SO_3^-$), carboxyl (-COOH), ethylene oxide ($-CH_2CH_2OH$), and poly(ethylene oxide) ($-(CH_2CH_2O)_5H$, PEO), was investigated, where permeabilities to acetate was suppressed in PEO-containing films in co-permeation with methanol. Here, we further examine this co-transport behavior in pendant PEO-containing films by preparing three chemically different crosslinked films with a constant crosslinker, poly(ethylene glycol) diacrylate (PEGDA), content and varied the remaining between a PEO-containing comonomer, poly(ethylene glycol) methacrylate (PEGMA), and a sulfonate-containing comonomer, 2-acrylamido-2-methyl-1-propanesulfonic acid (AMPS) (i.e. PEGDA-PEGMA, PEGDA-AMPS/PEGMA, and PEGDA-AMPS). For each chemistry, three structurally distinct films are prepared by varying pre-polymerization water content, leading to differences in water volume fraction (and thereby free volume). We observe the diffusivities of PEGMA-free films (PEGDA-AMPS) to acetate are increased in co-diffusion, while those of PEGMA-containing films (PEGDA-PEGMA and PEGDA-AMPS/PEGMA) to acetate are decreased. These results suggest the strategic addition of a charge-neutral pendant group in a charged IEMs is a valid approach to suppress the crossover of undesired molecules.

Keywords. Permeability; Multi-component transport; in situ ATR FTIR spectroscopy; Ion exchange membrane; PEGDA

1. Introduction

Understanding multi-component transport behavior in ion exchange membranes (IEMs) is of great interest for applications such as wastewater purification (i.e. electrodialysis [1,2]), energy storage devices (i.e. vanadium redox flow batteries [3]) and artificial photosynthesis devices (i.e. photoelectrochemical CO_2 reduction cells (PEC-CRCs) [4,5]). In particular, a major interest of PEC-CRCs is to design an IEM that minimize the crossover of CO_2 reduction products dissolved in catholyte, such as alcohols (e.g. methanol (MeOH) and ethanol) and carboxylate ions (e.g. formate and acetate (OAc^-)) [4,5]. Favorably, typical artificial photosynthesis devices do not require particularly high ionic conductivity [5], which often provides a higher degree-of-freedom upon tailoring the internal structure of the polymer matrix in a way that potentially minimizes the permeation of CO_2 reduction products in multi-component permeation.

Previously, our group observed a significant increase in OAc- permeability in co-permeation with MeOH in cation exchange membranes (CEMs), Nafion® 117 [6] and UV-crosslinked CEMs synthesized with a sulfonated monomer, 2-acrylamido-2-methylpropane sulfonic acid (AMPS) [7], and a crosslinker, poly(ethylene glycol) diacrylate (PEGDA, n = 13, where n represents the number of ethylene oxide repeat units). To rationalize this transport behavior, we proposed that a major contributor to this transport behavior is the charge screening by co-permeating MeOH (Fig. 1(F)), where co-diffusing MeOH suppresses the electrostatic repulsion (Donnan exclusion [8]) between bound sulfonate anions and mobile OAc^- anions [6,7,9]. Furthermore, we varied the AMPS content with charge-neutral comonomers with different chain lengths, acrylic acid (AA, n = 0), 2-hydroxyethyl methacrylate (HEMA, n = 1), and poly(ethylene glycol) methacrylate (PEGMA, n = 5) [10], where we observed increased OAc^- permeability in

membranes prepared with shorter comonomers (AA and HEMA), while it was suppressed in films prepared with longer comonomer (PEGMA) (Fig. 1(B)).

Here, to further investigate this multi-component transport behavior in charged polymer networks, we prepare a series of PEGMA-containing films by varying the PEGMA content with AMPS to understand the effect of this longer pendant chain (PEGMA) on multi-component transport behavior. For a better understanding, we have also varied the free volume [11] at each membrane composition by varying prepolymerization water content [12–14].

A pictorial description of how the presence of pendant PEGMA and co-diffusing MeOH could be suppressing the electrostatic repulsion between bound charge groups (sulfonates, SO_3^-) and mobile OAc^- is shown in Figure 1. In Figure 1(A-C), the diffusion of OAc^- by itself is depicted, where the mobile OAc^- experiences electrostatic repulsion from bound SO_3^- in CEMs (Fig. 1(C), ion-polymer interaction) and the interaction is being screened by the pendant PEG group (Fig. 1(B), polymer-polymer interaction). In Figure 1(D-F), the diffusion of OAc^- with MeOH is depicted, where the electrostatic repulsion is being screened by co-diffusing MeOH[6,7,9,15–17] and MeOH form a flux coupling [18] with OAc^- (Fig. 1(F), alcohol-polymer and ion-alcohol interactions). Further, the ion-alcohol flux coupling is being suppressed by pendant PEG group (Fig. 1(D,E), ion-alcohol-polymer interaction).

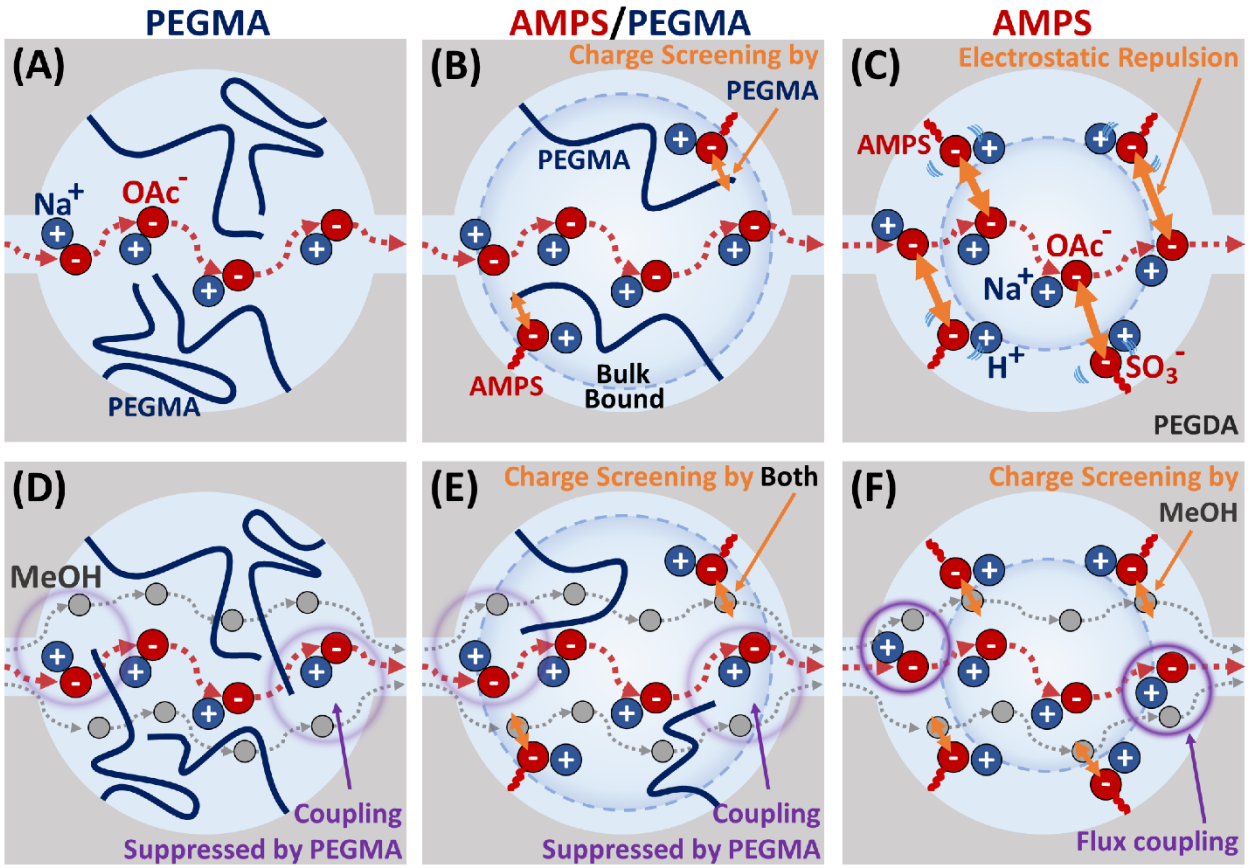

Fig. 1. Schematic depiction of NaOAc diffusion in (A,D) PEGDA-PEGMA, (B,E) PEGDA-AMPS/PEGMA, and (C,F) PEGDA-AMPS in (A-C) single and (D-F) co-diffusion with MeOH. Figures are reprinted from [7,9,10]with permission from Elsevier.

We measure permeabilities and solubilities of these films to MeOH and NaOAc in one- and two-component experiments and calculate diffusivities based on the solution-diffusion model (Eq. 1) to fully capture the transport behavior of this emergent transport behavior. As a dense membrane, molecular transport in IEMs is often described by the solution-diffusion model [19], which describes the overall solute transport is dependent on the sorption into the membrane and diffusion through the fractional free volume within the polymer matrix:

$$P_i = D_i K_i \tag{1}$$

where P_i is the permeability to solute i, D_i is the diffusivity to solute i, and K_i is the solubility to solute i. The permeability often changes in multi-solute transport as the presence of co-solutes affect both sorption (i.e. competitive sorption [20]) and diffusion (i.e. ion hydration [21] (free

89 volume theory [11,22]), flux coupling [9,18] and charge screening [9]). Here, the impact of a
90 pendant PEG chain (PEGMA) on the co-transport of two CO_2 reduction products (e.g. OAc^- and
91 MeOH) through a series of sulfonated PEGDA-AMPS-based films is studied.
92
93 **2. Experimental methods**
94 *2.1. Materials*
95 Methanol (MeOH, 99.8 %), sodium chloride (NaCl), sodium hydroxide beads (NaOH), and
96 phenolphthalein indicator solution were purchased from British Drug House (BDH®) Chemicals
97 (Poole, UK) and sodium acetate (NaOAc, 99 %) was purchased from ACS Chemical Inc. (Point
98 Pleasant, NJ). Poly(ethylene glycol) diacrylate (PEGDA, n = 13, where n represents the number
99 of ethylene glycol repeat units) and 2-acrylamido-2-methyl-1-propanesulfonic acid (AMPS, 99 %)
100 were purchased from Sigma-Aldrich Chemicals (St. Louis, MS). Poly(ethylene glycol)
101 methacrylate (PEGMA, n = 5) was purchased from Polysciences Inc. (Warrington, PA). 1-
102 Hydroxyl-cyclohexyl phenyl ketone (HCPK, photoinitiator) was purchased from Tokyo Chemical
103 Industry (Japan). All water used in this investigation was Type-1 deionized water produced by a
104 Waterpro BT Purification System from Labconco® (18.2 mΩ cm at 25 °C, 1.2 ppb TOC) (Kansas
105 City, MO).
106
107 *2.2. Film formation*
108 The detailed procedure on film formation is described in our previous work [7,10,13,14,23–26].
109 A total of 9 dissimilar membranes were prepared by UV-photopolymerization of
110 prepolymerization mixtures, as shown in Fig. 2 and Table 1. All membranes contain 68 mol% of
111 PEGDA (crosslinker) with the remaining 32 mol% varied between AMPS (A, comonomer) and

PEGMA (M, comonomer), namely PEGDA-PEGMA (-M, Fig. 2(A)), PEGDA-AMPS/PEGMA (-A/M, Fig. 2(B)), and PEGDA-AMPS (-A, Fig. 2(C)). Each composition was prepared with three different prepolymerization water contents, 20, 40, and 60 wt.%, and HCPK, 0.1 wt.% of polymer, as shown in Table 1. In the film name (#-X), # represents the wt.% of the prepolymerization water content and X represents the pendant groups (AMPS (A) and/or PEGMA (M)). For example, 40-A/M denotes the film prepared with PEGDA (68 mol%), AMPS (16 mol%), and PEGMA (16 mol%) with 40 wt.% of prepolymerization water content [7,13,14,23–26]. Essentially complete conversion has been determined as the mass of polymer network-forming monomers in the prepolymerization mixtures accords with the mass of the films after vacuum drying at 50 °C following 5 days of swelling in DI water within ~99 % [7,14,25,26].

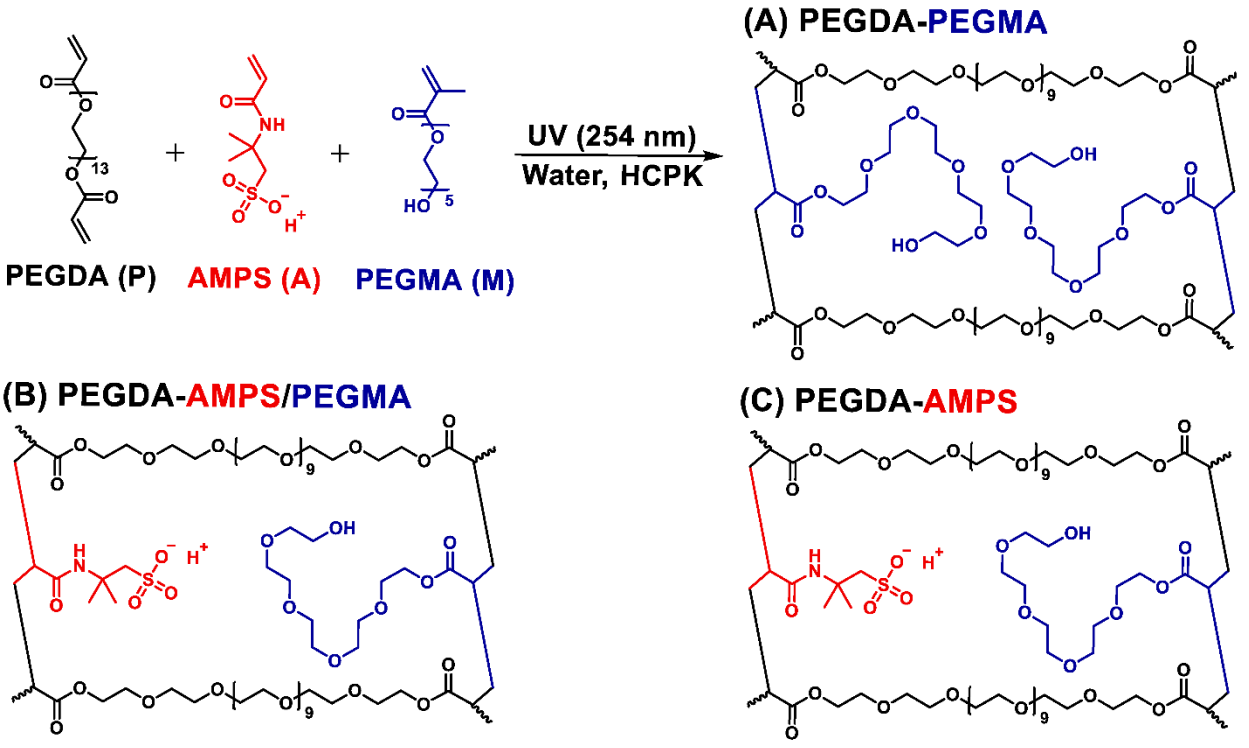

Fig. 2. Scheme of (A) PEGDA-PEGMA (-M), (B) PEGDA-AMPS/PEGMA (-A/M), and (C) PEGDA-AMPS (-A) films.

Table 1. Membrane properties from pre-polymerization mixtures

	AMPS[a] (mol%)	PEGMA[b] (mol%)	PEGDA (g)	AMPS (g)	PEGMA (g)	Water (g)	HCPK (g)
20-M	0	32	6.71	0.00	1.29	2.00	0.008
20-A/M	16	16	6.86	0.48	0.66	2.00	0.008
20-A	32	0	7.02	0.98	0.00	2.00	0.008
40-M	0	32	5.03	0.00	0.97	4.00	0.006
40-A/M	16	16	5.15	0.36	0.49	4.00	0.006
40-A	32	0	5.27	0.73	0.00	4.00	0.006
60-M	0	32	3.35	0.00	0.65	6.00	0.004
60-A/M	16	16	3.43	0.24	0.33	6.00	0.004
60-A	32	0	3.51	0.49	0.00	6.00	0.004

[a]AMPS = mol of AMPS/(mol of PEGDA + mol of AMPS + mol of PEGMA) × 100 %

[b]PEGMA = mol of PEGMA/(mol of PEGDA + mol of AMPS + mol of PEGMA) × 100 %

2.3. Ionic conductivity measurements

In-plane conductivity of all films was measured using a four-point conductivity cell (BekkTech BT-110) employed with a Gamry Interface 1000 potentiostat [7]. A rectangular section of the film (length: >1.0 cm, width: 0.5 cm, W) was cut and placed in the conductivity cell. The cell was then placed in water (500 mL), and electrochemical impedance spectroscopy (EIS) was performed after stabilization of the open circuit potential (frequency: 10 Hz-1 MHz, AC voltage: 10 mV). The EIS data has been analyzed in Gamry Echem Analyst software and the resistance, R (Ω), was obtained from the Nyquist plot. The ionic conductivity, σ, was measured as follows:

$$\sigma = \frac{L}{RWT} \tag{2}$$

where L, W, and T are the distance between two electrodes (0.5 cm), the width, and the thickness of the film, respectively.

2.4. Water content

Water uptake was measured gravimetrically. A 0.75-inch diameter hole punch was used to cut each hydrated film. The mass of the hydrated films, W_s, were measured after quickly blotting them

with tissue paper. The films were then dried under a vacuum at 50 °C for 24 hours and the mass of the dried film, W_d, measured [6]. The water uptake, ω_w, was calculated as follows:

$$\omega_w = \frac{W_s - W_d}{W_d} \cdot 100\% \tag{3}$$

where W_s is the mass of the swollen film and W_d is the mass of the dried film.

Film density was measured by buoyancy method with a density kit (ML-DNY-43, Mettler Toledo) coupled with a scale (ML204T, Mettler Toledo) [12]. The density, ρ_p, was calculated as follows:

$$\rho_p = (\rho_L - \rho_0)\left(\frac{W_0}{W_0 - W_L}\right) + \rho_0 \tag{4}$$

where ρ_L is the density of water (997.8 kg/m^3 at 22 ºC), ρ_0 is the density of air (1.225 kg/m^3), W_0 is the weight of the dried film in air, and W_L is the weight of the film in water.

Water volume fraction, ϕ_w, was calculated as follows:

$$\phi_w = \frac{(W_s - W_d)/\rho_L}{(W_s - W_d)/\rho_L + W_d/\rho_p} \tag{5}$$

2.5. Storage modulus

The storage modulus (*E*') of all compositions were measured by 3-point bending with a dynamic mechanical analyzer (DMA, TA Instruments RSA III) [27,28]. 2-mm spacers were used to prepare the all the films. After formation the films were then hydrated in a DI water for at least 5 days and the vacuum dried at 50 ºC for 24 hours. The dried films were then cut into rectangular shapes with a dimension of approximately 10×20 mm. The storage modulus of each film was then measured with a DMA at a heating rate of 1 ºC/min from 23 to 30 ºC (rubbery plateau) at a test frequency of 1 Hz.

164 *2.6. Ion Exchange Capacity*

165 Ion exchange capacity (IEC, mmol/g) was measured using a titration method [29–31]. A 2-inch
166 diameter hole punch was used to cut 3 hydrated films. The films were then dried in a vacuum oven
167 at 50 °C for 24 hours. The mass of the dried films, W_d, were measured. Each dried film was placed
168 in 1 M NaCl solution (50 mL) for 2 days. Next, 3 to 5 drops of phenolphthalein indicator were
169 added to each solution. Finally, 0.1 M NaOH solution was added dropwise until the color of the
170 solution remains pink. The IEC was measured as follows:

$$IEC = \frac{V_{NaOH} \times C_{NaOH}}{W_d} \tag{6}$$

171 where V_{NaOH} is the volume of NaOH solution added, C_{NaOH} is the concentration of the NaOH
172 solution (0.1 M), and W_d is the mass of the dried films.

173

174 *2.7. Sorption-desorption experiments*

175 The solubilities of each membrane to MeOH and NaOAc were measured for both single solutes
176 and for co-sorption in aqueous solutions by the sorption-desorption technique [6,7,32–34]. A 0.75-
177 inch diameter hole punch was used to cut 9 films from each membrane. Each film was then quickly
178 blotted with a tissue paper and immersed in a solution vial (15 mL), where a total of 9 solution
179 vials consists of three 1 M MeOH, three 1 M NaOAc, and three 1 M of each were prepared. All
180 films were placed in the solution vials for 3 days and the solution was replaced daily. A digital
181 caliper (±1 μm) was used to measure the film thickness by finding an average of five random
182 locations and ImageJ software (National Institutes of Health, MD) was used to calculate the area
183 of the films from digital photographs. Each film was then quickly blotted dry and immersed in a
184 vial of DI water (10 g) for 3 days. The solution from each vial was then transferred to a high-
185 performance liquid chromatography (HPLC) employed with a refractive index detector, Aminex

HPX-87H column (Bio-Rad, Hercules, CA) to determine the solute concentration in each desorption solution [34]. Briefly, the column temperature was maintained at 60 °C, the mobile phase was composed of 5 mM sulfuric acid in deionized water running at 0.55 mL/min, and the injected sample size was 10 μL. The solubility of each solute in the film was calculated as:

$$K_i = \frac{C_i^m}{C_i^s} \tag{7}$$

where C_i^s is the concentration of the solute i in the external solution (1 M) and C_i^m is the concentration of the solute *i* in the film, which is the product of the concentration of the solute *i* of the desorption solution and the volume of the desorption solution (10 mL) divided by the volume of solution-soaked films.

2.8. Diffusion cell experiments

A more detailed experimental method is thoroughly discussed elsewhere [7,9,10,12,33,34]. Briefly, MeOH and NaOAc permeabilities in hydrated films were measured using a temperature jacketed custom-built diffusion cell coupled with an in-situ ATR-FTIR probe (Mettler-Toledo ReactIR™ 15 with a shallow tip 9.5 mm DSun AgX DiComp probe) to detect the evolving MeOH and NaOAc concentration in the receiver cell. The feed cell was initially filled with either 1 M of MeOH, 1 M of NaOAc, or 1 M of each solute, while the receiver cell was initially filled with DI water. The time-resolved concentrations of each solute were measured from the time-resolved absorbances acquired from the solution in the receiver cell and fitted to Yasuda's model [35,36] to calculate the permeability. The osmotic diffusion of water from the receiver cell to the feed cell was neglected in this study as the difference due to osmotic diffusion was within the experimental error for identical solutions in Nafion® 117 [6].

3. Result and Discussion

A series of PEGDA-PEGMA (20, 40, 60-M), PEGDA-AMPS/PEGMA (20, 40, 60-A/M), and PEGDA-AMPS (20, 40, 60-A) films were prepared with varying water content in prepolymerization mixtures, 20, 40, and 60 wt.%, to investigate the effect of uncharged pendant comonomer, PEGMA (M), sulfonated pendant group, AMPS (A), and the free volume on solute and multi-component transport behavior. We evaluate the similarities and the differences in solubilities, permeabilities, and diffusivities of these polymer matrices in one- and two-component transport behavior.

3.1. Ionic conductivity, IEC, and water volume fraction

The ionic conductivity of the prepared membranes was measured yielding the results shown in Fig. 3(A) and Table 2. Ionic conductivities of all AMPS-free films (20, 40, 60-M) are zero, indicating they are not ionically conductive, as expected, due to the absence of charged moieties. The ionic conductivity of AMPS-containing films (20, 40, 60-A/M and -A) increases with increasing AMPS content. Similarly, the ion exchange capacity (IEC) of each film increases with increasing AMPS content as more counterions (H^+) are retained within the polymer matrix due to the membrane-bound sulfonates. Notably, the differences between measured and theoretical IEC of membranes are close, where the largest difference was observed in 40-A by 8 %, as shown in Table 2.

The water volume fraction of all films was measured as shown in Fig. 3(B) and Table 2. Generally, the water volume fraction was increased with increasing AMPS content. This is likely due to the increase in the water content as the hydration number (λ, H_2O/ion) of the sulfonate anion (12-16 [37]) is larger than that of the pendant PEG (n = 5) group (< 10 [38]). Moreover, the water volume fraction increases with increasing prepolymerization water content (from 20 to 60 wt.%). Similar behavior has been observed by Ju et al. [23], where the water volume fraction of

232 crosslinked PEGDA films prepared with 40 and 60 wt.% prepolymerization water content were
233 higher than that of the films prepared with 20 wt.% by 23 and 49 %. This is presumably due to a
234 reduction in crosslink density (as indicated from the storage modulus). Assuming the crosslinker
235 (PEGDA) and the photoinitiator (HCPK) are fully dissolved in solvent (water), the
236 prepolymerization mixture will become an isotropic hydrogel, where the crosslinks will be evenly
237 dispersed through the film and, therefore, free volume elements (initially filled with water) will
238 also be evenly dispersed.

239 The ionic conductivities increase with increasing water volume fractions; see Fig. 3 (C).
240 This is partially linked with Robeson's upper bound relationship for CEMs [39], which explains
241 the transport of protons within the negatively-charged CEMs are limited by the amount of water
242 within the polymer network because the free volume element (as represented by the water volume
243 fraction) is the transport medium for protons and the films with less amount of the free volume
244 element will allow less number of protons to transport [12,13,23,31].
245

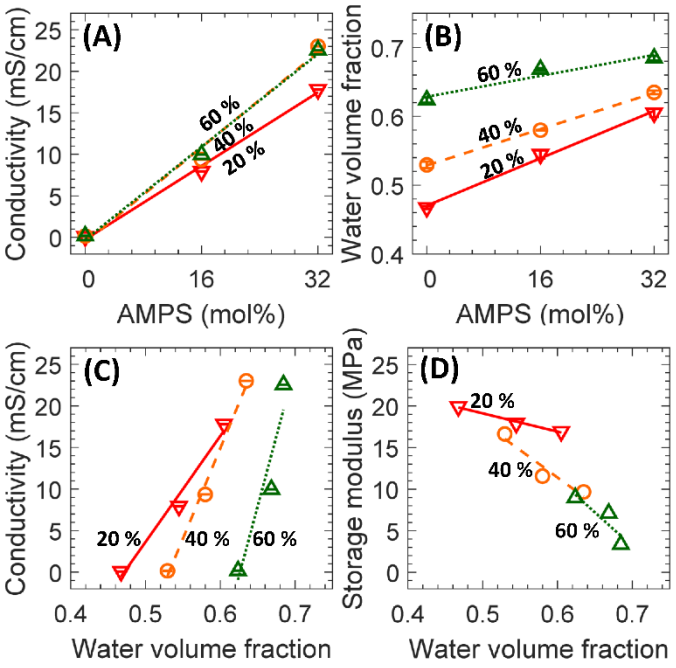

Fig. 3. (A) Ionic conductivities and (B) water volume fractions of all films, 0 (M), 16 (A/M), and 32 mol% (-A) of AMPS content, prepared with 20 (▽, red, solid line), 40 (○, orange, dashed) and 60 wt.% (△, green, dotted) of prepolymerization water content. (C) Ionic conductivities to water volume fractions. (D) Storage modulus to water volume fractions. Each data point is the average of 3 membranes with error bars corresponding to the standard deviation. Lines are present as a guide to the eye.

Table 2. Ionic conductivity, ion exchange capacity, water volume fraction, storage modulus of all films

	AMPS (mol%)	Conductivity (σ, mS/cm)	Theoretical IEC (meq/g dry polymer)[a]	Measured IEC (meq/g dry polymer)	Water volume fraction	Storage modulus (MPa)
20-M	0	0 ± 0	-	-	0.467 ± 0.002	19.9
20-A/M	16	8 ± 0	0.29	0.32 ± 0.00	0.545 ± 0.006	17.9
20-A	32	18 ± 0	0.59	0.60 ± 0.01	0.605 ± 0.006	16.9
40-M	0	0 ± 0	-	-	0.529 ± 0.005	16.6
40-A/M	16	9 ± 0	0.29	0.32 ± 0.00	0.580 ± 0.000	11.6
40-A	32	23 ± 0	0.59	0.62 ± 0.00	0.635 ± 0.003	9.7
60-M	0	0 ± 0	-	-	0.624 ± 0.004	9.0
60-A/M	16	10 ± 0	0.29	0.34 ± 0.01	0.668 ± 0.002	7.1
60-A	32	23 ± 0	0.59	0.60 ± 0.01	0.685 ± 0.003	3.4

[a]Theoretical IEC = mmol of AMPS/(mass of PEGDA + mass of AMPS + mass of comonomer)

3.2. Dynamic mechanical analysis

The storage modulus of all films at the rubbery plateau is shown in Fig. 3(D) and Table 2. Generally, the storage modulus of the films decreases with increasing the prepolymerization water content. For instance, the storage moduli of the films prepared with 20 wt.% prepolymerization water content are higher than those of with 40 and 60 wt.% prepolymerization water content by 1.4 and 2.8 times, on average. Moreover, the storage modulus of the films decreases with increasing AMPS content. For example, the storage moduli of the films prepared without AMPS (20, 40, 60-M), is higher than those of with 16 and 32 mol% AMPS contents (20, 40, 60-A/M and -A), by 1.2 and 1.5 times, on average.

The storage modulus of a crosslinked film is a proxy to understand the crosslink density (crosslinks per unit volume, mol/cm^3) of the film [40]. For instance, Flory's rubber elasticity relationship is often utilized as a proxy to the crosslink densities, ν_e, of the films [40]:

$$\nu_e = \frac{E'}{3RT} \tag{8}$$

where *E'* is the storage modulus (MPa), *R* is the gas constant (8.314 cm^3 MPa/K mol), and *T* is the temperature (298.15 K). This relationship suggests the crosslink density of the films decrease with either increasing prepolymerization water content [13,23,41] or with increasing AMPS content [14,25]. Lastly, as the free volume often increases with a decreasing the crosslink density, the water volume fraction is a reasonable proxy to estimate the free volume within these films [13,23,41]; see Fig. 4(D).

3.3. Single and Multi-solute Permeability

The diffusive permeabilities of all membranes to MeOH and NaOAc in single and co-permeation were measured via diffusion cell experiments; see Supporting information Figure S1 for exemplary

concentration-versus-time plots. Extracted permeability values using the Yasuda model [35,36] are shown in Supporting information Table S2, Figure S2, and Fig. 4; where Fig. 4(A) and (B) are scaled differently. Negligible membrane swelling was observed during all permeability measurements, as measured by the changes in membrane thickness; see Supporting Information Table S3.

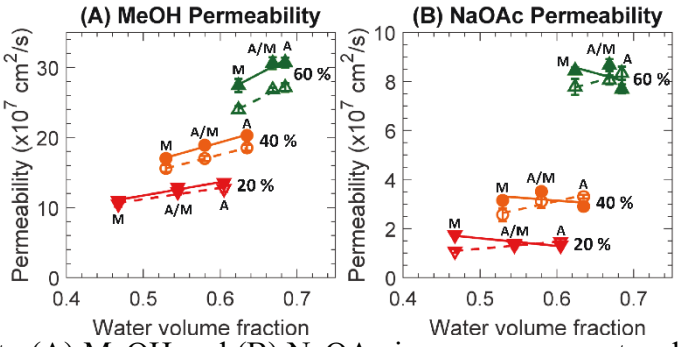

Fig. 4. Permeabilities to (A) MeOH and (B) NaOAc in one-component, solid lines with (red), ● (orange), and ▲ (green) for 20, 40, and 60 wt.% of prepolymerization water contents, respectively, and two-component, dashed lines with ▽ (red), ○ (orange), and △ (green) for 20, 40, and 60 wt.% of prepolymerization water content, respectively. M, A/M, and A denote films prepared with 0, 16, and 32 mol% of AMPS contents, respectively. Each data point is the average of 3 experiments with error bars corresponding to the standard deviation. Lines are present as a guide to the eye.

Generally, permeabilities to MeOH were consistent with the relative water volume fraction of the corresponding membrane films [7,10,12,24], suggesting that the permeation of MeOH is strongly dependent on the free volume and less dependent on the type of pendent groups (PEGMA and/or AMPS). In co-permeation with NaOAc, MeOH permeability was decreased in all films. For instance, MeOH permeabilities of films prepared with 20, 40, and 60 wt.% water content in co-permeation were decreased by 1.05, 1.09, and 1.12 times, respectively, on average. To rationalize this behavior, we conjectured a competitive diffusion[9,10,12,17,33,34,42], which describes the diffusional path of a fast-diffusing solute can be interfered with by a slow-diffusing co-solute and has to move around it. Higher decreases in MeOH permeabilities of films prepared

with higher prepolymerization water content (and thereby free volume) could thereby be a result of increased interaction as the permeation of NaOAc increases.

Generally, permeabilities to NaOAc were distinctly increased in films prepared with higher water contents. NaOAc permeabilities of films prepared with 40 and 60 wt.% were higher than those of films prepared with 20 wt.% water content by 1.2 and 2.2 times, respectively, on average. A contribution to these increases in NaOAc permeabilities is due to the difference in NaOAc solubilities, where the solubilities of these films were increased with the increasing prepolymerization water content and correspondingly the water volume fractions of the film. NaOAc permeabilities were about 5 times smaller than MeOH permeabilities on average. This behavior is partially due to diffusion [24] as the kinetic diameter of MeOH (3.6 Å [43]) is smaller than the hydrated diameters of dissociated ions, such as Na^+ ion (7.16 Å [44]) and OAc^- ion (7.44 Å [45,46]).

In co-permeation, NaOAc permeabilities were increased in PEGMA-free films (20, 40, 60-A) by 1.11 times, on average, while they were decreased in PEGMA-containing films (20, 40, 60-M and -A/M) by 1.15 times on average. This increased permeability in -A films is possibly a result of the flux coupling [6,7,10,12] where the diffusion of NaOAc is facilitated by a fast-diffusing MeOH upon a flux coupling. Another contribution is the charge screening by MeOH [9,17], which is a conjecture that the electrostatic interaction between bound charge group and mobile ion can be suppressed by co-diffusing alcohol. However, these are likely not the only contributing phenomena as other factors (hydration number of dissociated ions [16,47], feed concentration [6], relative permittivity [48,49], etc.) can also have a role in this emergent behavior. The observed decrease in permeability of PEGMA-containing films (20, 40, 60-M and -A/M) to NaOAc in co-permeation is potentially a consequence of the flux coupling between MeOH and NaOAc being

suppressed by the pendant PEO from PEGMA (solute-solute-chain interaction). Similar behavior has been observed in a previous investigation [10] where NaOAc permeabilities of films with long pendant PEO side chains were consistent in co-permeation with MeOH, while those of films with a shorter pendant group (carboxyl or ethylene oxide) were significantly increased in co-permeation. This conjected solute-solute-chain interaction in the co-permeation of NaOAc will further be discussed in the following section.

3.5. Single and Multi-solute Solubility

The solubilities of MeOH and NaOAc in all films are shown in Supporting information Table S4, Figure S2, and Fig. 5. Membrane volumes were calculated before and after the sorption experiments by measuring the film thickness, the average of 5 random locations measured with a digital caliper (± 1 μm), and the area, a digital photograph coupled with ImageJ software (National Institutes of Health, MD) [25]; see Supporting information Table S1 for values. While all films did not experience significant swelling or deswelling during sorption experiments to MeOH [7,24], they experienced slight deswelling during sorption experiments to NaOAc, where the degree of deswelling increases with an increase in AMPS content. For instance, the average volumetric deswelling of PEGDA-PEGMA (20, 40, 60-M), PEGDA-AMPS/PEGMA (20, 40, 60-A/M), and PEGDA-AMPS (20, 40, 60-A) films after sorption in 1 M NaOAc containing solutions were 1.05, 1.11, and 1.16 times, respectively. This osmotic deswelling is due to the presence of the acetate salts leading to the transport of water out of the membrane at varying degrees due to the presence of membrane-bound ions (AMPS) within the membrane. [6,32].

In single sorption, MeOH solubilities of films generally increase with increasing water volume fraction, see Fig. 5(A). For instance, MeOH solubilities of the films prepared with 20 wt.%

of prepolymerization water content are less than those with 40 and 60 wt.% of the prepolymerization water content by 1.08 and 1.26 times, respectively, on average. Moreover, MeOH solubilities of films prepared without AMPS (20, 40, 60-M) are less than those with 16 (20, 40, 60-A/M) and 32 mol% of AMPS content (20, 40, 60-A) by 1.06 and 1.13 times, respectively, on average. Similar behavior has been reported by Galizia et al., where they observed MeOH solubilities (Sorption solutions: 0.1-12 M) of crosslinked PEGDA films (prepared with 0, 20, and 60 wt.% of prepolymerization water contents) to be increased with increasing water content [24]. This indicates the MeOH-polymer interaction is less favorable than the MeOH-water interaction in sorption.

We observe a different behavior in co-sorption with NaOAc, where MeOH solubilities of the films prepared with 20 wt.% of prepolymerization water content are less than those with 40 and 60 wt.% of prepolymerization water content by 1.09 times and 1.07 times, respectively, on average. Also, MeOH solubilities of the films prepared in absence of AMPS are less than those with 16 and 32 mol% of AMPS content by 1.13 and 1.08 times, respectively, on average. This indicates the MeOH-polymer interaction is less apparent in co-sorption.

In single sorption, NaOAc solubilities of films generally increase with increasing prepolymerization water content, where films prepared with 20 wt.% of prepolymerization water content are less than those with 40 and 60 wt.% prepolymerization water content by 1.67 and 3.04 times, respectively, on average. Similar behavior has been reported by Jang et al., where they observed solubilities (for sorption solutions of 0.01-1 M) of crosslinked PEGDA films (prepared with 0, 20, and 40 wt.% of prepolymerization water contents) to various salts (i.e. NaCl, KCl, and LiCl) to increase with increasing water content [27]. This indicates the NaOAc-polymer interaction is less favorable than the NaOAc-water interaction in sorption. On the other hand, NaOAc

373 solubilities of films are generally decreased with increasing AMPS content, where films prepared
374 without AMPS have higher solubilities than those with 16 and 32 mol% of the AMPS content by
375 1.08 and 1.13 times, respectively, on average. Similar behavior has been reported by Yan et al,
376 where they observed the solubilities (for sorption solutions of 0.01-1 M) of crosslinked PEGDA-
377 AMPS films (prepared by varying PEGDA to AMPS ratio at a constant prepolymerization water
378 content, 25 wt.%) to NaCl to decrease with increasing AMPS content [25]. This indicates the
379 NaOAc-polymer interaction is significant, as the electrostatic repulsion (Donnan exclusion [8])
380 between bound sulfonate anions (AMPS) and mobile acetate anions (OAc^-) is considerable. The
381 effect of electrostatic interactions between a negatively-charge ion (chloride) and a charged
382 segment (sulfonate) in crosslinked PEGDA-AMPS membranes has also been investigated by Yu
383 et al. [50], where they found the increasing electrostatic interactions in strongly charged
384 membranes, such as those examined herein, led to decreased chloride solubility. For very strongly
385 charged membranes both the ideal Donnan equilibrium model [8] and Manning's limiting law [51]
386 were able to capture this behavior, while a polyelectrolyte non-random two-liquid (NRTL) model
387 [52], which included both long-range electrostatic interactions (polyion-ion and ion-ion) and short-
388 range interactions [53], was better able to capture the behavior across varied membrane charge
389 content and external solution salt content. The reduced solubility of OAc- in the AMPS-containing
390 films (20, 40, 60-A and-A/M) is thereby attributable to the analogous electrostatic interactions
391 between the negatively-charged OAc- and bound sulfonate.
392 We observe similar behavior in co-sorption with MeOH, where NaOAc solubilities of the
393 films prepared with 20 wt.% of prepolymerization water content are less than those with 40 and
394 60 wt.% of prepolymerization water content by 1.85 times and 3.07 times, respectively, on average.
395 Also, NaOAc solubilities of the films prepared in absence of AMPS was higher than those with 16

and 32 mol% of AMPS content by 1.02 and 1.17 times, respectively, on average. This is an indication that MeOH has a negligible impact on the NaOAc-polymer interaction in sorption.

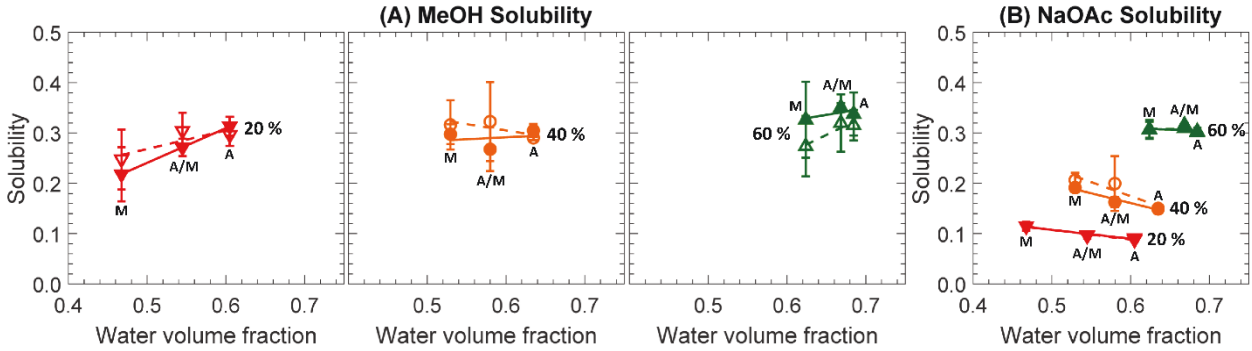

Fig. 5. Solubilities to (A) MeOH and (B) NaOAc in one-component, solid lines with (red), ● (orange), and ▲ (green) for 20, 40, and 60 wt.% of prepolymerization water contents, respectively, and two-component, dashed lines with ▽ (red), ○ (orange), and △ (green) for 20, 40, and 60 wt.% of prepolymerization water content, respectively. M, A/M, and A denote films prepared with 0, 16, and 32 mol% of AMPS contents, respectively. Each data point is the average of 3 experiments with error bars corresponding to the standard deviation. Lines are present as a guide to the eye.

3.6. Single and Multi-solute Diffusivity

The diffusivities of all prepared membranes to MeOH and NaOAc in single and co-diffusion are calculated using Eq. (1), dividing measured permeabilities by measured solubility. Calculated diffusivities are shown in Supporting information Table S5, Figure S2, and Fig. 6; where Fig. 6(A) and (B) are scaled differently. The Mackie-Meares model [54] was used to estimate the MeOH and NaOAc diffusivities in these films, which states:

$$D_i = D_{o,i}\left(\frac{\phi_w}{2-\phi_w}\right)^2 \tag{9}$$

where D_i is the diffusivity of a membrane to solute i, ϕ_w is the water volume fraction, and $D_{0,i}$ is the solute diffusivity in pure water (1.49×10^{-5} cm^2/s for MeOH [55] and 1.21×10^{-5} cm^2/s for NaOAc[9,56,57]). The model tends to better fit data for salts over other small molecules as Mackie and Meares initially devised the model to estimate the salt diffusivities [54]. As a result, the model has better agreement with NaOAc diffusivities over MeOH diffusivities (Fig. 6), where similar

behaviors were reported elsewhere [9,17,24,58]. Additionally, this model neglects the solute-polymer interactions and treats polymer chains as impenetrable obstacles [54]. In the case of NaOAc diffusivities, the model tends to fit better with PEGMA-containing films (20, 40, 60-M and -A/M), which we take as an indication that the NaOAc-polymer interaction (solute-polymer) is lessened in these films over PEGMA-free films (20, 40, 60-A); see Fig. 6(B).

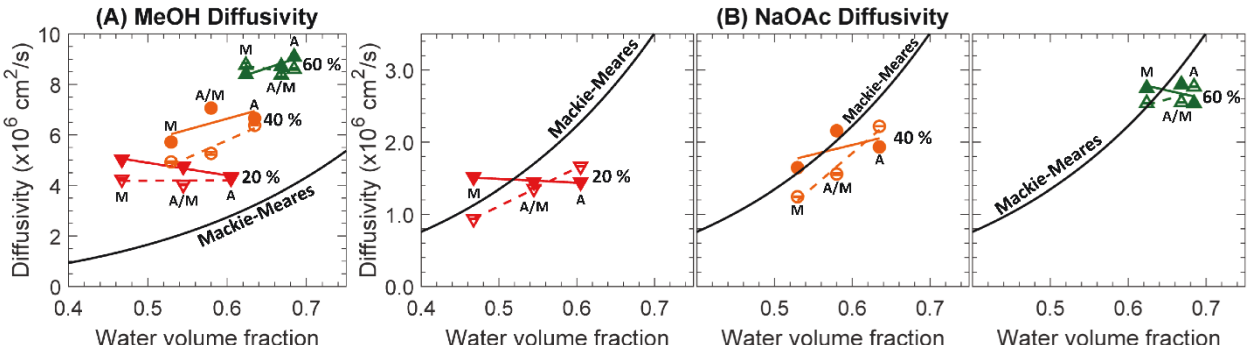

Fig. 6. Diffusivities to (A) MeOH and (B) NaOAc in one-component, solid lines with (red), ● (orange), and ▲ (green) for 20, 40, and 60 wt.% of prepolymerization water contents, respectively, and two-component, dashed lines with ▽ (red), ○ (orange), and △ (green) for 20, 40, and 60 wt.% of prepolymerization water content, respectively. M, A/M, and A denote films prepared with 0, 16, and 32 mol% of AMPS contents, respectively. Lines are present as a guide to the eye. Mackie-Meares' fits for each solute are shown in solid lines.

Generally, MeOH diffusivities increase with increasing water volume fractions. For instance, MeOH diffusivities of the films prepared with 20 wt.% prepolymerization water content (20-M, A/M, A) are less than those with 40 and 60 wt.% prepolymerization water content (40- and 60-M, A/M, A) by 1.4 and 1.9 times, respectively, on average, in single diffusion. Similar behavior has been reported by Galizia et al., where they observed MeOH diffusivities (for feed solutions of 0.1-12 M) of crosslinked PEGDA films (prepared with 0, 20, and 60 wt.% of prepolymerization water contents) to increase with increasing water content [24]. Similar to single solute diffusivities, MeOH diffusivities of 20- films are less than those of 40- and 60- films by 1.3 and 2.0 times, respectively, on average, in co-diffusion with NaOAc. Interestingly, MeOH diffusivities of the films prepared with 20 wt.% of water content decrease sightly with decreasing AMPS content

within the films, while those of the films prepared with either 40 or 60 wt.% of water content increase with increasing AMPS content; see Fig.6 (A). One possible cause of this behavior is the pendant sulfonate group may act as a bulky obstruction, especially at a low water volume fraction. However, this behavior requires further investigation.

In co-diffusion, MeOH diffusivities of the films prepared with 20 and 40 wt.% decrease by 1.12 and 1.17 times, respectively, on average; see Fig. 6(A). We reported similar behavior in both CEMs [9] and anion exchange membranes [17]. To rationalize this behavior, we conjectured the diffusional path of fast-diffusing MeOH being obstructed by slow-diffusing NaOAc (Competitive diffusion). Here, we augment this conjecture such that this co-diffusive behavior remains consistent in films with longer, pendant PEO chains. Interestingly, MeOH diffusivities of the films prepared with both PEGMA and AMPS (-A/M) are higher than those with either PEGMA (-M) or AMPS (-A) in single diffusion, but -A/M diffusivities to MeOH are less than -M and -A diffusivities in co-diffusion. One possibility is a steric effect between PEGMA and AMPS (chain-chain interaction) that is in favor of the diffusion of MeOH. However, the impact of chain-chain interactions might be suppressed in co-diffusion as the diffusant-diffusant interaction (competitive diffusion) is more apparent on the diffusion of MeOH. On the other hand, MeOH diffusivities of the films prepared with 60 wt.% in co-diffusion are essentially the same as those in single diffusion. This indicates the competitive diffusion is more apparent in films with less water volume fraction (free volume).

Similar to MeOH diffusivities, NaOAc diffusivities increase with increasing water volume fraction. For instance, NaOAc diffusivities of 20- films are less than those of 40- and 60- films by 1.3 and 1.8 times, respectively, on average, in single diffusion. Similar behavior has been reported by Jang et al., where they observed diffusivities (for feed solutions of 0.01-1 M) of crosslinked

463 PEGDA films (prepared with 0, 20, and 40 wt.% prepolymerization water content) to various salts
464 (i.e. NaCl, KCl, and LiCl) to increase with increasing water content [58]. Again, NaOAc
465 diffusivities of 20- films are less than those of 40- and 60- films by 1.3 and 2.0 times, respectively,
466 on average, in co-diffusion with MeOH. Moreover, NaOAc diffusivities of the films prepared with
467 20 wt.% of water content decrease with decreasing AMPS content within the films; see Fig.6 (B).
468 Again, this is presumably due to the pendant sulfonate group act as a blocking group to suppress
469 the solute diffusion.

470 For the films prepared with 20 and 40 wt.% prepolymerization water content, NaOAc
471 diffusivities of -M films and -A/M films decrease by 1.4 and 1.2 times, respectively, on average,
472 and those of -A films increase by 1.2 times, on average, in co-diffusion with MeOH; see Fig. 6(B).
473 We reported the increase of NaOAc diffusivities in co-diffusion with MeOH in CEMs [6,9]. To
474 rationalize this behavior, we conjectured the electrostatic repulsion (Donnan exclusion [8])
475 between bound sulfonate anions and mobile OAc^- is screened by co-diffusing MeOH (Charge
476 screening by co-diffusant, [6,9,10,16]); see Fig. 1(F). Recently, Katzenberg et al. investigated the
477 water-alcohol interaction in Nafion (commercial CEM), where they suggested alcohols may
478 penetrate between the water and polymer interfaces as the alcohol-polymer affinity is stronger than
479 the water-polymer affinity (non-uniform distribution of water-alcohol in CEM) [59]. This can be
480 a contribution to suppress the electrostatic interaction between OAc^- and polymer ($sulfonate^-$), as
481 the alcohol (less polar)-polymer (less polar) affinity can be stronger than the OAc^-(polar)-polymer
482 affinity. The decrease of NaOAc diffusivities in co-diffusion with MeOH is an emergent transport
483 behavior. Previously, we reported the NaOAc permeabilities of 20-M and 20-A/M being consistent
484 in co-permeation with MeOH, while those of analogous films prepared with a shorter comonomer
485 (either acrylic acid or hydroxyethyl methacrylate) were significantly increased in co-permeation

with MeOH [10]. To rationalize this behavior, we conjectured (1) the electrostatic repulsion between bound sulfonate and OAc^- is screened by long pendant PEO chains even in single permeation (charge screening by chains, Fig. 1(B)) and (2) flux coupling with co-permeating MeOH has been suppressed by long pendant PEO chains (Fig. 1(D,E)). Here, we augment these conjectures as diffusion-based transport behaviors. Moreover, the results from this investigation validate the addition of a charge-neutral pendant group in a charged IEM as a valid strategic approach to suppress the crossover of undesired molecules (i.e. MeOH and OAc^- in CO_2 reduction cells).

For 60- films, NaOAc diffusivities of -M films and -A/M films decrease by 1.1 and 1.1 times, respectively, on average, and those of -A films increase by 1.1 times, on average, in co-diffusion; see Fig. 6(B). This indicates both the electrostatic repulsion (sulfonate-OAc^-) and the flux coupling (MeOH-NaOAc) are more apparent in films with less water volume fraction (free volume). While these new findings may serve as practical tools for designing target-specific membranes, more fundamental investigations (i.e. Maxwell-Stefan [60], dielectric constant [61], internal structure [13,62], etc.) can be valuable to fully capture these complex multicomponent transport behaviors in IEMs.

4. Conclusions

A series of PEGDA-PEGMA (-M), PEGDA-AMPS/PEGMA (-A/M), and PEGDA-AMPS (-A) films with varied prepolymerization water contents (20, 40, and 60 wt.%) were prepared. Water volume fractions and ionic conductivities are measured to describe the transport behavior within these AMPS-free dense membranes (-M) and AMPS-containing cation exchange membranes (-A/M and -A). Permeabilities and solubilities to MeOH and NaOAc are measured in one- and two-

component diffusion cell experiments and diffusivities are calculated from the solution-diffusion relationship. In one-component transport, both MeOH and NaOAc permeabilities are increased with increasing water volume fractions. However, NaOAc permeabilities of PEGMA-free films (-A) to NaOAc are increased and those of PEGMA-containing films (-M and -A/M) are decreased in co-permeation with MeOH. We postulate that the introduction of both diffusant-diffusant interactions (MeOH-NaOAc) and diffusant-diffusant-chain interactions (MeOH-NaOAc-PEGMA) leads to these changes in permeation behavior and that the presence of the pendant PEGMA side chains is principally responsible for this emergent behavior by suppressing the electrostatic repulsions between bound sulfonate anions and mobile OAc^-. Lastly, for both MeOH and OAc- we find the primary driver in differences in membrane permeability to be through changes in diffusion compared to changes in sorption behavior. Additional insights from computational approaches to simulate these multi-component transport or the development of experimental approaches to probe this behavior are needed. Overall, this investigation advances a preliminary understanding of how varied membrane physiochemical properties lead to differences in emergent transport behavior for charged polymer networks challenged with solutes and complex mixtures of solutes.

Acknowledgements

This material is based upon work supported by the National Science Foundation under Grant No. 1936146. JMK, AM, and BSB also acknowledge the support for this work provided by the Auburn University Presidential Awards for Interdisciplinary Research Program.

CRediT

Jung Min Kim: Conceptualization, Methodology, Investigation, Validation, Formal analysis, Writing - original draft, Visualization. **Antara Mazumder:** Investigation. **Jing Li:** Investigation. **Zhihua Jiang:** Resources. **Bryan S. Beckingham:** Conceptualization, Methodology, Resources, Writing - review & editing, Supervision, Project administration, Funding acquisition.

Appendix A. Supplementary material

Supplementary data associated with this article can be found in the online version at

References

[1] M. Grzegorzek, K. Majewska-Nowak, A.E. Ahmed, Removal of fluoride from multicomponent water solutions with the use of monovalent selective ion-exchange membranes, Sci Total Environ. 722 (2020) 137681. https://doi.org/10.1016/j.scitotenv.2020.137681.

[2] T. Benvenuti, M. García-Gabaldón, E.M. Ortega, M.A.S. Rodrigues, A.M. Bernardes, V. Pérez-Herranz, J. Zoppas-Ferreira, Influence of the co-ions on the transport of sulfate through anion exchange membranes, J Membrane Sci. 542 (2017) 320–328. https://doi.org/10.1016/j.memsci.2017.08.021.

[3] A.R. Crothers, R.M. Darling, D.I. Kushner, M.L. Perry, A.Z. Weber, Theory of Multicomponent Phenomena in Cation-Exchange Membranes: Part III. Transport in Vanadium Redox-Flow-Battery Separators, J Electrochem Soc. 167 (2020) 013549. https://doi.org/10.1149/1945-7111/ab6725.

[4] M.R. Singh, A.T. Bell, Design of an artificial photosynthetic system for production of alcohols in high concentration from CO 2, Energ Environ Sci. 9 (2015) 193–199. https://doi.org/10.1039/c5ee02783g.

[5] M. Krödel, B.M. Carter, D. Rall, J. Lohaus, M. Wessling, D.J. Miller, Rational Design of Ion Exchange Membrane Material Properties Limits the Crossover of CO 2 Reduction Products in Artificial Photosynthesis Devices, Acs Appl Mater Inter. 12 (2020) 12030–12042. https://doi.org/10.1021/acsami.9b21415.

[6] B.S. Beckingham, N.A. Lynd, D.J. Miller, Monitoring multicomponent transport using in situ ATR FTIR spectroscopy, J Membrane Sci. 550 (2018). https://doi.org/10.1016/j.memsci.2017.12.072.

[7] J.M. Kim, B.M. Dobyns, R. Zhao, B.S. Beckingham, Multicomponent transport of methanol and acetate in a series of crosslinked PEGDA-AMPS cation exchange membranes, J Membrane Sci. (2020) 118486. https://doi.org/10.1016/j.memsci.2020.118486.

[8] F.G. Helfferich, Ion Exchange, Dover, 1995.

[9] J.M. Kim, B.S. Beckingham, Transport and co-transport of carboxylate ions and alcohols in cation exchange membranes, J Polym Sci. (2021). https://doi.org/10.1002/pol.20210383.

[10] J.M. Kim, B.S. Beckingham, Comonomer effects on co-permeation of methanol and acetate in cation exchange membranes, Eur Polym J. (2021) 110307. https://doi.org/10.1016/j.eurpolymj.2021.110307.

[11] R.W. Baker, Membrane Technology and Applications, (2018). https://doi.org/10.1002/9781118359686.

[12] B.M. Dobyns, J.M. Kim, B.S. Beckingham, Multicomponent transport of methanol and sodium acetate in poly(ethylene glycol) diacrylate membranes of varied fractional free volume, Eur Polym J. 134 (2020) 109809. https://doi.org/10.1016/j.eurpolymj.2020.109809.

[13] H. Ju, A.C. Sagle, B.D. Freeman, J.I. Mardel, A.J. Hill, Characterization of sodium chloride and water transport in crosslinked poly(ethylene oxide) hydrogels, J Membrane Sci. 358 (2010) 131–141. https://doi.org/10.1016/j.memsci.2010.04.035.

[14] A.C. Sagle, H. Ju, B.D. Freeman, M.M. Sharma, PEG-based hydrogel membrane coatings, Polymer. 50 (2009) 756–766. https://doi.org/10.1016/j.polymer.2008.12.019.

[15] P. Parise, A.A. Jr, B. Parekh, Reverse osmosis: chlorine-resistant polysulfone reverse osmosis membrane and module, Ultrapure Water. (1987).

[16] G.M. Geise, D.R. Paul, B.D. Freeman, Fundamental water and salt transport properties of polymeric materials, Prog Polym Sci. 39 (2014) 1–42. https://doi.org/10.1016/j.progpolymsci.2013.07.001.

[17] J.M. Kim, S.B. Chakrapani, B.S. Beckingham, Tuning Compositional Drift in the Anionic Copolymerization of Styrene and Isoprene, Macromolecules. (2020). https://doi.org/10.1021/acs.macromol.0c00526.

[18] K.A. Thompson, R. Mathias, D. Kim, J. Kim, N. Rangnekar, J.R. Johnson, S.J. Hoy, I. Bechis, A. Tarzia, K.E. Jelfs, B.A. McCool, A.G. Livingston, R.P. Lively, M.G. Finn, N-Aryl-linked spirocyclic polymers for membrane separations of complex hydrocarbon mixtures., Sci New York N Y. 369 (2020) 310–315. https://doi.org/10.1126/science.aba9806.

[19] J.G. Wijmans, R.W. Baker, The solution-diffusion model: a review, J Membrane Sci. 107 (1995) 1–21. https://doi.org/10.1016/0376-7388(95)00102-i.

[20] R.T. Chern, W.J. Koros, B. Yui, H.B. Hopfenberg, V.T. Stannett, Selective permeation of CO2 and CH4 through kapton polyimide: Effects of penetrant competition and gas-phase nonideality, J Polym Sci Polym Phys Ed. 22 (1984) 1061–1084. https://doi.org/10.1002/pol.1984.180220610.

[21] H.M.A. Rahman, G. Hefter, R. Buchner, Hydration of Formate and Acetate Ions by Dielectric Relaxation Spectroscopy, J Phys Chem B. 116 (2011) 314–323. https://doi.org/10.1021/jp207504d.

[22] M.L. Greenfield, D.N. Theodorou, Geometric analysis of diffusion pathways in glassy and melt atactic polypropylene, Macromolecules. 26 (1993) 5461–5472. https://doi.org/10.1021/ma00072a026.

[23] H. Ju, B.D. McCloskey, A.C. Sagle, V.A. Kusuma, B.D. Freeman, Preparation and characterization of crosslinked poly(ethylene glycol) diacrylate hydrogels as fouling-resistant membrane coating materials, J Membrane Sci. 330 (2009) 180–188. https://doi.org/10.1016/j.memsci.2008.12.054.

[24] M. Galizia, D.R. Paul, B.D. Freeman, Liquid methanol sorption, diffusion and permeation in charged and uncharged polymers, Polymer. 102 (2016) 281–291. https://doi.org/10.1016/j.polymer.2016.09.010.

[25] N. Yan, D.R. Paul, B.D. Freeman, Water and ion sorption in a series of cross-linked AMPS/PEGDA hydrogel membranes, Polymer. 146 (2018) 196–208. https://doi.org/10.1016/j.polymer.2018.05.021.

[26] H. Lin, E.V. Wagner, J.S. Swinnea, B.D. Freeman, S.J. Pas, A.J. Hill, S. Kalakkunnath, D.S. Kalika, Transport and structural characteristics of crosslinked poly(ethylene oxide) rubbers, J Membrane Sci. 276 (2006) 145–161. https://doi.org/10.1016/j.memsci.2005.09.040.

[27] E.-S. Jang, J. Kamcev, K. Kobayashi, N. Yan, R. Sujanani, T.J. Dilenschneider, H.B. Park, D.R. Paul, B.D. Freeman, Influence of water content on alkali metal chloride transport in cross-linked Poly(ethylene glycol) Diacrylate.1. Ion sorption, Polymer. 178 (2019) 121554. https://doi.org/10.1016/j.polymer.2019.121554.

[28] S. Kalakkunnath, D.S. Kalika, H. Lin, B.D. Freeman, Segmental Relaxation Characteristics of Cross-Linked Poly(ethylene oxide) Copolymer Networks, Macromolecules. 38 (2005) 9679–9687. https://doi.org/10.1021/ma051741t.

[29] T.M. Lim, M. Ulaganathan, Q. Yan, Advances in Batteries for Medium and Large-Scale Energy Storage, Part Four Des Issues Appl. (2015) 477–507. https://doi.org/10.1016/b978-1-78242-013-2.00014-5.

[30] G.M. Geise, B.D. Freeman, D.R. Paul, Characterization of a sulfonated pentablock copolymer for desalination applications, Polymer. 51 (2010) 5815–5822. https://doi.org/10.1016/j.polymer.2010.09.072.

[31] X.C. Chen, J.B. Kortright, N.P. Balsara, Water Uptake and Proton Conductivity in Porous Block Copolymer Electrolyte Membranes, Macromolecules. 48 (2015) 5648–5655. https://doi.org/10.1021/acs.macromol.5b00950.

[32] G.M. Geise, L.P. Falcon, B.D. Freeman, D.R. Paul, Sodium chloride sorption in sulfonated polymers for membrane applications, J Membrane Sci. 423 (2012) 195–208. https://doi.org/10.1016/j.memsci.2012.08.014.

[33] B.M. Carter, B.M. Dobyns, B.S. Beckingham, D.J. Miller, Multicomponent transport of alcohols in an anion exchange membrane measured by in-situ ATR FTIR spectroscopy, Polymer. 123 (2017). https://doi.org/10.1016/j.polymer.2017.06.070.

[34] B.M. Dobyns, J.M. Kim, J. Li, Z. Jiang, B.S. Beckingham, Multicomponent transport of alcohols in Nafion 117 measured by in situ ATR FTIR spectroscopy, Polymer. (2020) 123046. https://doi.org/10.1016/j.polymer.2020.123046.

[35] H. Yasuda, C.E. Lamaze, L.D. Ikenberry, Permeability of solutes through hydrated polymer membranes. Part I. Diffusion of sodium chloride, Die Makromolekulare Chemie. 118 (1968) 19–35. https://doi.org/10.1002/macp.1968.021180102.

[36] H. Yasuda, A. Peterlin, C.K. Colton, K.A. Smith, E.W. Merrill, Permeability of solutes through hydrated polymer membranes. Part III. Theoretical background for the selectivity of dialysis membranes, Die Makromolekulare Chemie. 126 (1969) 177–186. https://doi.org/10.1002/macp.1969.021260120.

[37] A. Kusoglu, A.Z. Weber, New Insights into Perfluorinated Sulfonic-Acid Ionomers, Chem Rev. 117 (2017) 987–1104. https://doi.org/10.1021/acs.chemrev.6b00159.

[38] H. Schott, Extent of Hydration of Ethers in Aqueous Solution., J Chem Eng Data. 11 (1966) 417–418. https://doi.org/10.1021/je60030a039.

[39] L.M. Robeson, H.H. Hwu, J.E. McGrath, Upper bound relationship for proton exchange membranes: Empirical relationship and relevance of phase separated blends, J Membrane Sci. 302 (2007) 70–77. https://doi.org/10.1016/j.memsci.2007.06.029.

[40] P.J. Flory, Principles of Polymer Chemistry, Cornell University Press, 1953.

[41] H. Lin, T. Kai, B.D. Freeman, S. Kalakkunnath, D.S. Kalika, The Effect of Cross-Linking on Gas Permeability in Cross-Linked Poly(Ethylene Glycol Diacrylate), Macromolecules. 38 (2005) 8381–8393. https://doi.org/10.1021/ma0510136.

[42] B. Pan, B. Xing, Competitive and Complementary Adsorption of Bisphenol A and 17α-Ethinyl Estradiol on Carbon Nanomaterials, J Agr Food Chem. 58 (2010) 8338–8343. https://doi.org/10.1021/jf101346e.

[43] T. Borjigin, F. Sun, J. Zhang, K. Cai, H. Ren, G. Zhu, A microporous metal–organic framework with high stability for GC separation of alcohols from water, Chem Commun. 48 (2012) 7613–7615. https://doi.org/10.1039/c2cc33023g.

[44] E.R. Nightingale, Phenomenological Theory of Ion Solvation. Effective Radii of Hydrated Ions, J Phys Chem. 63 (1959) 1381–1387. https://doi.org/10.1021/j150579a011.

[45] R. Caminiti, P. Cucca, M. Monduzzi, G. Saba, G. Crisponi, Divalent metal–acetate complexes in concentrated aqueous solutions. An x-ray diffraction and NMR spectroscopy study, J Chem Phys. 81 (1984) 543–551. https://doi.org/10.1063/1.447336.

[46] Hitoshi. Ohtaki, Tamas. Radnai, Structure and dynamics of hydrated ions, Chem Rev. 93 (1993) 1157–1204. https://doi.org/10.1021/cr00019a014.

[47] V.N. Afanas'ev, Solvation of Electrolytes and Nonelectrolytes in Aqueous Solutions, J Phys Chem B. 115 (2011) 6541–6563. https://doi.org/10.1021/jp1108834.

[48] K. Chang, H. Luo, G.M. Geise, Water content, relative permittivity, and ion sorption properties of polymers for membrane desalination, J Membrane Sci. 574 (2019) 24–32. https://doi.org/10.1016/j.memsci.2018.12.048.

[49] K. Chang, H. Luo, G.M. Geise, Influence of Salt Concentration on Hydrated Polymer Relative Permittivity and State of Water Properties, Macromolecules. 54 (2021) 637–646. https://doi.org/10.1021/acs.macromol.0c02188.

[50] Y. Yu, N. Yan, B.D. Freeman, C.-C. Chen, Mobile ion partitioning in ion exchange membranes immersed in saline solutions, J Membrane Sci. 620 (2020) 118760. https://doi.org/10.1016/j.memsci.2020.118760.

[51] G.S. Manning, Limiting Laws and Counterion Condensation in Polyelectrolyte Solutions I. Colligative Properties, J Chem Phys. 51 (1969) 924–933. https://doi.org/10.1063/1.1672157.

[52] Y. Yu, Y. Li, N. Hossain, C.-C. Chen, Nonrandom two-liquid activity coefficient model for aqueous polyelectrolyte solutions, Fluid Phase Equilibr. 497 (2019) 1–9. https://doi.org/10.1016/j.fluid.2019.05.009.

[53] Y. Song, C.-C. Chen, Symmetric Electrolyte Nonrandom Two-Liquid Activity Coefficient Model, Ind Eng Chem Res. 48 (2009) 7788–7797. https://doi.org/10.1021/ie9004578.

[54] J.S. Mackie, P. Meares, The diffusion of electrolytes in a cation-exchange resin membrane I. Theoretical, Proc Royal Soc Lond Ser Math Phys Sci. 232 (1955) 498–509. https://doi.org/10.1098/rspa.1955.0234.

[55] L. Hao, D.G. Leaist, Binary Mutual Diffusion Coefficients of Aqueous Alcohols. Methanol to 1-Heptanol, J Chem Eng Data. 41 (1996) 210–213. https://doi.org/10.1021/je950222q.

[56] E.E. Hills, M.H. Abraham, A. Hersey, C.D. Bevan, Diffusion coefficients in ethanol and in water at 298K: Linear free energy relationships, Fluid Phase Equilibr. 303 (2011) 45–55. https://doi.org/10.1016/j.fluid.2011.01.002.

[57] P. Vany´sek, Ionic Conductivity and Diffusion at Infinite Dilution, CRC Handbook of Chemistry and Physics, 93rd Edition. (2012).

[58] E.-S. Jang, J. Kamcev, K. Kobayashi, N. Yan, R. Sujanani, T.J. Dilenschneider, H.B. Park, D.R. Paul, B.D. Freeman, Influence of water content on alkali metal chloride transport in cross-linked Poly(ethylene glycol) diacrylate.2. Ion diffusion, Polymer. 192 (2020) 122316. https://doi.org/10.1016/j.polymer.2020.122316.

[59] A. Katzenberg, A. Angulo, A. Kusoglu, M.A. Modestino, Impacts of Organic Sorbates on the Ionic Conductivity and Nanostructure of Perfluorinated Sulfonic-Acid Ionomers, Macromolecules. 54 (2021) 5187–5195. https://doi.org/10.1021/acs.macromol.1c00494.

[60] M. Soltanieh, S. Sahebdelfar, Interaction effects in multicomponent separation by reverse osmosis, J Membrane Sci. 183 (2001) 15–27. https://doi.org/10.1016/s0376-7388(00)00554-8.

[61] K. Chang, G.M. Geise, Dielectric Permittivity Properties of Hydrated Polymers: Measurement and Connection to Ion Transport Properties, Ind Eng Chem Res. 59 (2019) 5205–5217. https://doi.org/10.1021/acs.iecr.9b03950.

[62] G.M. Geise, C.M. Doherty, A.J. Hill, B.D. Freeman, D.R. Paul, Free volume characterization of sulfonated styrenic pentablock copolymers using positron annihilation lifetime spectroscopy, J Membrane Sci. 453 (2014) 425–434. https://doi.org/10.1016/j.memsci.2013.11.004.